

# Development of High-brightness Diode Laser Pump Modules for LIDAR Applications

Todd Rose, David Hinkley, Jerome Fuller, James Swenson and Renny Fields  
The Aerospace Corporation  
PO Box 92957  
Los Angeles, California 90009

Tuomo Konnunaho, Jukka Kongas, Tiina Amberla, and Mervi Koskinen  
Coherent Tutcore Ltd  
P. O. Box 48  
FIN-33721 Tampere, Finland

Mark Mondry, Jim Harrison, and Paul Rudy  
Coherent Semiconductor Division  
5100 Patrick Henry Drive  
Santa Clara, CA 95054-1112

**Abstract**-Laser diode pump modules are being developed to enable efficient longitudinal pulsed pumping of solid-state lasers. Optimization of such devices entails near micron positional alignment between elements of a diffraction limited GaP lens array and an identically pitched array of 200 single mode laser emitters. Production issues such as diode array "smile" (vertical bowing) and thermal expansion mismatch between the diode array and its heat sink have induced systematic errors compromising the final product. Through precise emitter-to-emitter spacing measurement techniques, this problem has been characterized and a solution using either silicon carbide or copper tungsten as the submount has been developed and tested. Initial tests indicate acceptable performance for developing fully stacked devices. Additional spacing optimization and emitter improvements should lead to the program achieving its goal of developing a 15% electrically efficient 600 W peak power fully collimated stack within a 1 cm by 1 cm package at TRL 4.

## Introduction

The development of high peak-power lasers is increasingly needed to support Earth science missions. ICESAT, launched this year and Calypso, to be launched in Fall '04 are the first

extended earth observing laser missions planned by NASA. Several other high priority laser-based missions to measure water vapor, ozone and tropospheric wind are still being aggressively pursued but have been delayed in part because of the high cost of flying large payloads. Improving laser efficiency could reduce payload size, weight and power requirements, thereby improving reliability and minimizing cost.

The efficiency of a laser is dependent upon several factors, as illustrated in Figure 1. Many improvements in power conditioning, diode

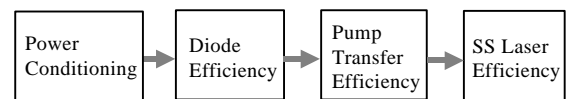
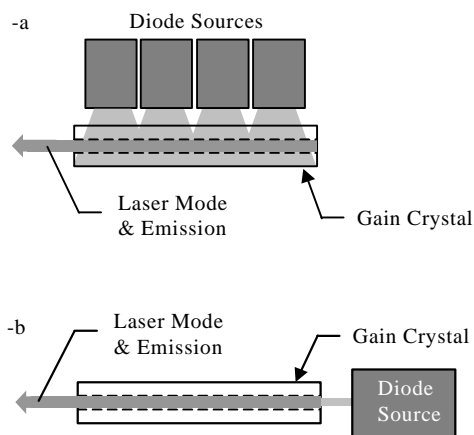


Figure 1. Contributors to laser efficiency

efficiency, nonlinear processes and solid-state laser operation have already been or are being pursued for implementation in laser payloads. A remaining area where significant device improvement could be realized is in the transfer of optical pump energy to the laser crystal. To our knowledge, no current or proposed pulsed laser missions have electrical efficiencies that exceed 6% (ICESAT engineering model<sup>1</sup>). One could obtain a 2.5-4 fold improvement in laser

performance irrespective of the host material by changing the flight-standard pump configuration from a transverse geometry to a longitudinal one as depicted in Figure 2. The longitudinal configuration can operate more efficiently since the pump light is captured and confined within the laser mode and not lost in the “surrounding” laser material.



**Figure 2. a) Transverse versus b) longitudinal laser pumping with laser diodes.**

The Aerospace Corporation has investigated longitudinal pumping for improving the efficiency of solid-state laser devices for space applications<sup>2-5</sup> for many years. Our previous efforts were focused on continuous wave solid-state lasers. The work discussed here began three years ago and has focused on QCW (quasi-continuous wave) solid-state lasers to accommodate missions requiring high peak energy sources. Our goal is to develop a pump module that integrates large arrays (bars of 200 emitters) of single-mode diffraction-limited devices with arrays of micro-lenses to yield a collimated pump source. This work is a collaboration between The Aerospace Corporation and the Coherent Semiconductor Division and was initially reported in these proceedings two years ago<sup>6</sup>. In these proceedings, we will present the most recent progress in the development of the pump devices.

## Emitter Development

At the conclusion of the first year's effort, testing of 2.5, 3.5 and 4.5 $\mu$ m width devices suggested that 4.5 $\mu$ m stripe widths would be the best compromise for this application. While the emission from the 4.5 $\mu$ m stripes is not strictly diffraction limited, it can be efficiently collected and collimated by our f/0.7 microlens and transferred to an acceptable spot size in the far field. Although we sacrifice beam quality, we gain margin in reliability by reducing the optical intensity per emitter. Similarly, the choice of 200 emitters per cm (instead of 100) effectively limits the peak power per emitter to 300 mW for a 60W goal per bar. Other issues addressed in this work are the control of emitter-to-emitter wavelength variation, reducing the fast axis divergence and improving the stripe definition process to achieve increased device reproducibility and reliability. In Figure 3 and 4, respectively, we compare the diode spectra before and after wafer treatments that are designed to control wavelength spread of the single-mode devices. In Figure 5, we show results from EPI modification to reduce fast axis divergence.

The ability to repeatedly grow high efficiency material has brought into question the optimum path for emitter definition. Throughout the early period of this effort, the laser devices were produced through a self-aligned structure (SAS) process. In this process a lateral index step is defined by overgrowth on a groove. It has good contact area but critical cavity dimensions are determined by epitaxial control. For the final growths of this project, the best SAS growths will be compared to ridge waveguides, where the emitter is defined by etching away material lateral to the emitter. These have low contact area but entail only a single growth for the emitter. To date we have not produced devices which have an optimum balance of low divergence, wavelength control and high slope efficiency.

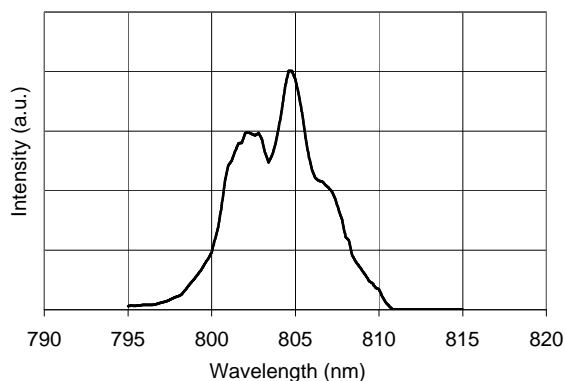


**Figure 3. Diode bar spectrum with unprocessed back facet.**

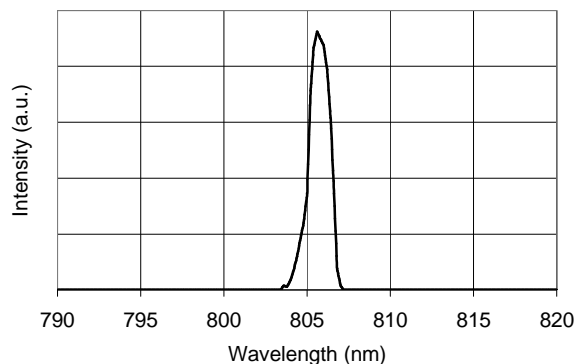


**Figure 4. Diode bar spectrum with back facet processed for improved wavelength control.**

### Lens Fabrication

We can produce 200-element aspheric lens arrays in GaP where each lenslet has a focal length of 100  $\mu\text{m}$  and numerical apertures of 0.75 and 0.25 in the fast and slow axes, respectively. We can reliably saw the arrays into 0.7 mm high strips that are easily glued to a laser diode bar sub-mount. Issues remaining involve improving in-house equipment to enable greater lens fabrication throughput. A new, larger area ion-mill will come online near the conclusion of this ATIP effort.

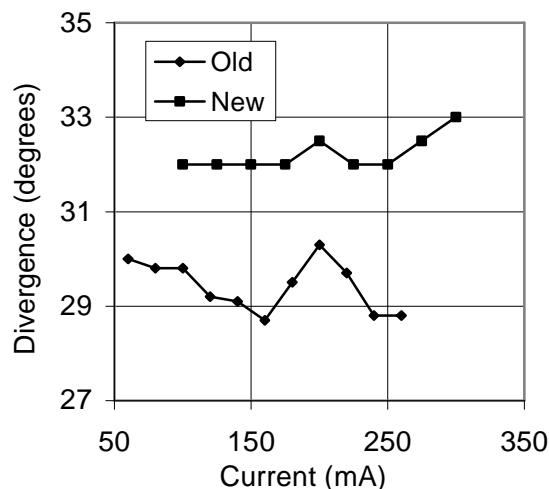


**Figure 5. Modified EPI for fast axis divergence control.**

### Integration Issues and Lens/Bar Results

#### *Pitch Errors*

Initial attempts to align lens arrays to diode bars and focus the collimated spot resulted in an astigmatic beam. It was postulated that the bar and lens pitch were not matched despite both components being manufactured from precise masks. This problem is depicted in Figure 6.

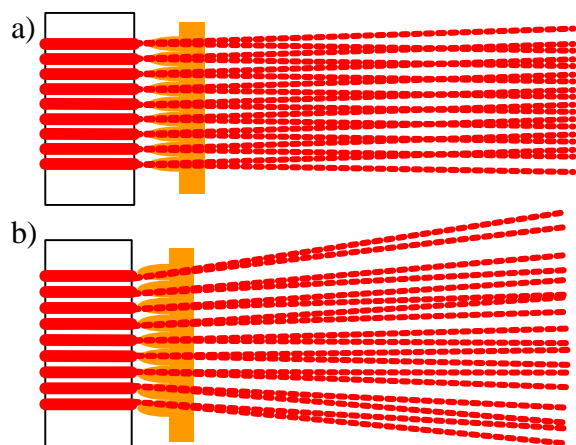


**Figure 6. Pitch variation between lens array and diode bar: (a) ideal case with parallel beamlets; (b) observed case with unparallel beamlets**

**Table 1. Thermal, mechanical, and electrical properties of various candidate submount materials.**

Property	Units	copper	CVD SiC	BeO	Cu/W	6061-T6	GaAs
electrical resistance	Ohm cm <sup>2</sup> /cm	10 <sup>-6</sup>	10 <sup>-2</sup>	10 <sup>14</sup>	10 <sup>-5</sup>	10 <sup>-6</sup>	
thermal conductivity	W/mK	391	250	250	200	167	55
elastic modulus	x 10 <sup>6</sup> lb/in <sup>2</sup>	17	68	50	40	10	12
coeff. thermal expansion	x 10 <sup>-6</sup> /°C	17	2.2	8	6.5	23	5.8

After several tests were conducted, it was determined that the lens pitch was accurate but the diode bar emitter pitch had contracted significantly. It is believed that the contraction results from the process used to bond the GaAs bar to the copper mount. As shown in Table 1, there is a significant coefficient of thermal expansion (CTE) mismatch between copper and GaAs. Analysis of the expected contraction is consistent with the magnitude and direction of the measured results. Using the apparatus depicted in Figure 7, we measured the position of each emitter for several copper-mounted devices and determined the average total accumulated error across the devices to be  $7 \pm 2$   $\mu\text{m}$ . Furthermore, we observed that the contraction was not evenly distributed but occurred more in the middle of the bar than on the ends.

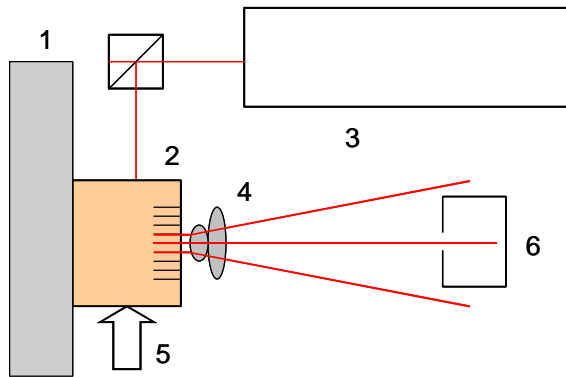


**Figure 7. Diagram of emitter spacing measurement station: 1) reference straight edge; 2) diode bar; 3) interferometer; 4) microscope objective; 5) sub-micron linear motor; 6) slit aperture power meter.**

Two approaches were pursued to reduce the effect of diode bar contraction. The first approach used a redesigned diode mask with a slightly enlarged pitch to pre-compensate for the subsequent contraction during the bonding process. A set of diode bars was fabricated with an overall increase in length of 7  $\mu\text{m}$  over the nominal. The emitter position error measurement for a precompensated diode bar bonded to a copper mount is shown in Figure 8. There is a significant improvement. While the precompensated laser diode bar spacing reduced the overall emitter-to-emitter spacing error, this method does not improve on the other problems such as making them flat and reducing their susceptibility to bending if mishandled.

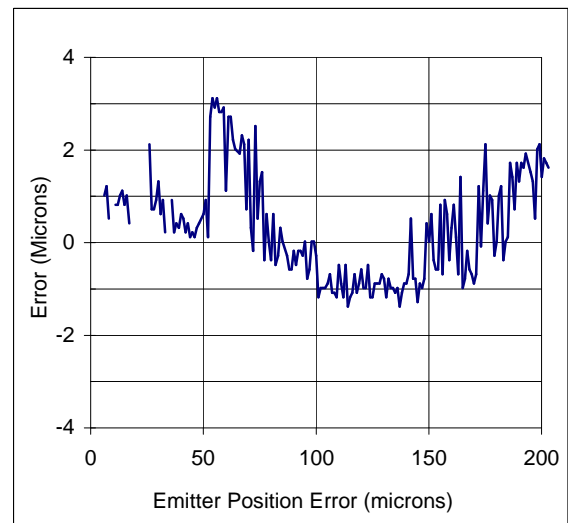


**Figure 8. Emitter spacing measurements of a precompensated diode bar on a copper mount.**

In the second approach, we sought to reduce the emitter-to-emitter spacing error by choosing a material for the diode mount that had a closer CTE match with GaAs. We also wanted a

material that would better maintain its flatness. SiC was chosen for these reasons. SiC diode mounts, fabricated by Morgan Advanced Ceramics, were bonded to uncompensated diode bars. The emitter spacing results are shown in Figure 9. Because the CTE of SiC is less than GaAs, the diode bars actually expanded. This gave us confidence that the CTE mismatch was the main cause of the diode bar pitch variations. We are currently fabricating mounts from 10/90 CuW which has an even closer CTE to GaAs, but an unknown flatness quality.

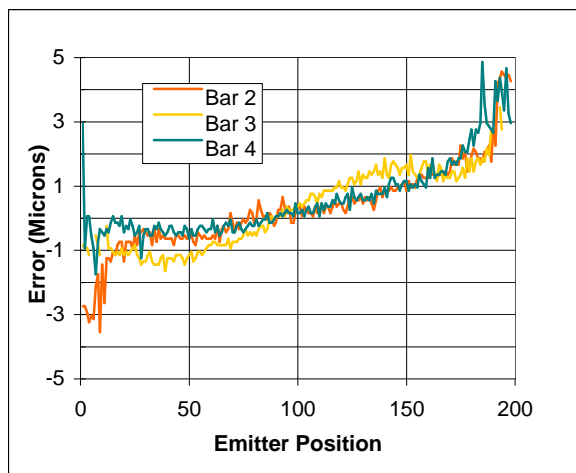


**Figure 9. Emitter spacing measurements of a 200-emitter uncompensated bar bonded to SiC mount.**

#### *Smile Errors*

The smiles of several diode bars with both copper and SiC mounts were measured using an imaging system with a CCD camera. Smile is the RMS vertical deviation of the emitters from a flat line. The results are shown in Table 2. The diode bars mounted on SiC had far less smile than those mounted on copper. The reason is that SiC is easier to lap flat and does not permanently deform during handling.

**Table 2. Smile measurements for uncompensated SiC mounted bars and pitch adjusted Copper mounted bars.**

SiC mount		Cu mount	
Bar #	Smile ( $\mu\text{m}$ )	Bar #	Smile ( $\mu\text{m}$ )
1	1.0	8	3.4
2	0.7	9	2.2
3	1.7	16	1.2
4	0.5	20	4.6
5	1.0	22s	0.9
		22t	1.2
		24	1.2
		26	3.9
		84	0.9
Avg. = 1.0		Avg. =2.2	

#### *Current versus Light*

The current versus optical output power for the SiC mounted bars is shown in Figure 10. The bars are pulsed at 100 Hz with a 200  $\mu\text{S}$  pulse duration. There is no power degradation due to the lower thermal conductivity of SiC. The same measurement for the precompensated diode bars mounted on copper mounts is shown in Figure 11.

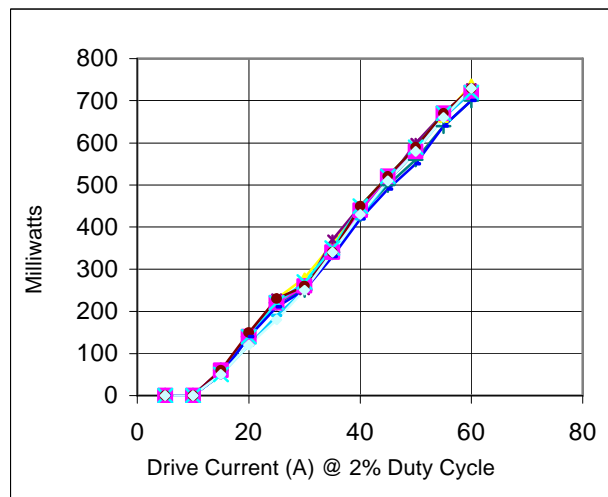


**Figure 10. L-I curve for SiC lot #1, bars 1-5.**

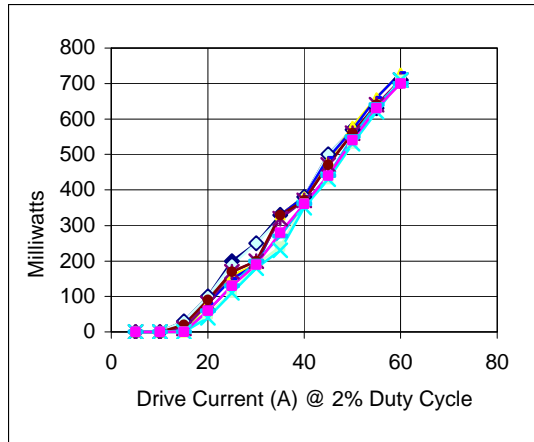


**Figure 11. L-I curve for precompensated lot #1, bars 1-5.**

#### *Bar and Lens Alignment*

Spiricon images were taken to assess the optical performance of the diode bar and lens arrays. In Figure 12, we display a far field image obtained with a lens array and a SiC mounted bar. The collimated output was then focused with an 8-cm lens to a spot which was approximately 2x the diffraction limited. The position of the focused spot is shorter than the lens focal length because the emitter pitch error still remains. Additional improvement should be obtained from the 10/90 CuW diode mounts that will be tested shortly.

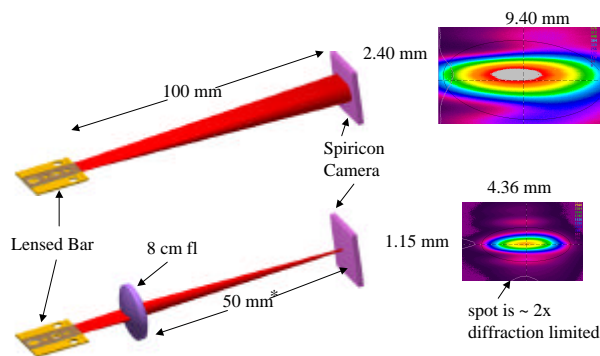


**Figure 12. SiC Bar integrated with 200 element microlens array.**

#### **Future Plans**

As a result of our recent efforts, we have developed a viable approach for achieving a high-efficiency pump module that will reach an electrical-to-optical conversion efficiency of 50%. Our next step is to stack ten lensed diode bar arrays to yield a 600W peak power pump laser for Nd:YAG.

#### **References:**

1. R. A. Afzal, GSFC, ICESAT CDR and personal communication
2. R. A. Fields, M. Birnbaum, and C. L. Fincher, "Highly Efficient Nd:YVO<sub>4</sub> Diode Laser End-Pumped Solid-State Lasers", *Appl. Phys. Lett.* **51**, 1885 (1987)
3. R. A. Fields, M. Birnbaum, and C. L. Fincher, "15.8% Efficient Diode-Laser End-Pumped Nd:YVO<sub>4</sub> Laser", *CLEO Post Deadline Digest*, (1988) pp. 460
4. T. S. Rose, J. S. Swenson, D. Hinkley and R. A. Fields, "Efficient Laser Performance Using a Micro-Optic Based Pump source", *Advanced Solid State Lasers*, **20**, 276 (1994)
5. H. Asonen, A. Ovthinnikov, G. Zhang, J. Nappi, P. Savolainen, and M. Pessa, "Aluminum-Free 980-nm GaInAs/GaInAsP/GaInP Pump Lasers", *IEEE J. Quant. Elect.* **30**, 415 (1994)
6. R. Fields et al., *Proceedings of the Earth Science Technology Conference 2001*, College Park, Maryland paper B1P4